A Novel Beamforming Approach to Stereo Sound

Samuel Rohrer

Abstract

The goal of this ongoing project is to determine the best method of creating stereo sound and separation within the footprint of a tablet in the near-field (less than six feet from the user). Beamforming (creating directional wavefronts) was used to achieve this; however, the best method of near-field beamforming was unknown. Three techniques were simulated and compared using MATLAB: point and sum (a new method developed during research), delay and sum beamforming, and no beamforming. Simulation results showed that point and sum beamforming was the superior method. This technique was then tested in hardware. To do this, the logic for the processing was defined using VHDL and synthesized onto a Field Programmable Gate Array (FGPA). On a high-level, this processing circuitry samples all audio inputs and then transfers the data to a matrix of registers. The data was then selected from the registers based on the delays that had already been calculated to create the beamforming. Results suggest the system is functioning correctly by separating the sound as many users have confirmed. It is clear point and sum beamforming is the best method for near-field beamforming and that stereo separation can be created in the footprint of a tablet.

1. Introduction

This research aims to take a novel approach to creating an audio image within the footprint of a tablet by evaluating the different methods of beamforming and then applying the chosen method to a speaker system. Audio images occur in headphones due to stereo isolation, which is defined as complete separation between the two stereo channels. Simply defined, an audio image allows the user to perceive events occurring without using visual cues. Although beamforming has been a part of radar systems for many years, it has only recently seen use in acoustic applications. As of now the two main applications of acoustic beamforming are: sound bars used in home theaters that use some beamforming to create a faux surround sound effect, and large conference room microphones that isolate individual speakers. However, there are no commercial products that utilize beamforming to create stereo isolation within the footprint of a tablet. Furthermore, there is no established research setting out a methodology for attempting beamforming in such a small field of space.

Currently, there is not a sufficient amount of research into acoustic beamforming techniques. This necessitates reliance on previous research in other fields of beamforming to assess the current state of this field of research. There are many different ideas pertaining to the actual implementation of beamforming; however, most have some basic similarities. The vast majority of these implementations are based on delay and sum beamforming - which is the idea of inserting different time delays at each driver so that a single directed wave-front can be created and controlled by changing the time delays and thus how these waves sum in the field. Beamforming allows an array of receivers or transmitters to function as a single larger receiver or transmitter (Greenwood, 2011). The receiver or transmitter can be changed by simply changing the beamforming pattern, which allows unique signal control opportunities (Greenwood, 2011). Furthermore, the beamforming image is created by these phase shifts and integrated over the array (receivers or transmitters) being used (Simonetti & Huang, 2009). However, this is just a conceptual idea of how beamforming works. In reality there are much more complex mathematical ideas at play. A key idea is that of Minimum Variance, proposed for use in Photoacoustic Imaging by Park, Karpiouk, Aglyamov, and Emelianov (2008), which aims to reduce off-axis signals and therefore increase the accuracy of the signals being transmitted. Additionally, Lagrange multipliers and covariance matrices can be used to perform spatial smoothing (Park, Karpiouk, Aglyamov, & Emelianov, 2008), although with a photoacoustic

image, which is not the acoustic image that this research aims to address. In another instance beamforming was used to measure depth in a horizontal waveguide; the experimenters attempted to maximize the signal to noise ratio (Hinich, 1977). To find sound pressures over the area of the field, the wave equation was solved; then, using statistical analysis and Gaussian distributions, changing wave values over time could be predicted and calculated (Hinich, 1977). Although there are many positive reviews of beamforming, an article on the creation of "sound bullets" deplores beamforming for being reliant on actuators and its use of "cumbersome and application specific drivers" (Spadoni, Daraio, & Freund, 2010).

The methods described to implement beamforming so far have been similar because all are variations of delay and sum beamforming. It has proved successful because uses of such beamforming abound. For instance, beamforming is common in the radar and communication systems of military aircraft to accurately place Radio Frequency (RF) waves in new Active Electronically Scanned Arrays (Manz, 2012). Variations of these arrays have evolved themselves into radar inferometers, which are used to map landscapes below the array and utilize beamforming to aid with these measurements (Deller et al., 2011). Other terms used are, "beam shaping" or "cross-strapping;" both refer to beamforming and its use in the communication satellite INTELSAT VI (Pollack & Weiss, 1984). Beamforming was also used to determine the directionality of surface-generated noise in an upward refracting ocean by measuring the wave in each plane (Buckingham, 1994). In another medical study, a MEG (magneto encephalography) used beamforming to produce "rich frequency information" (Hagan et al., 2009). These examples show the relevance of beamforming to both civilian and military applications.

All of these articles discuss methods of achieving far-field beamforming with delay and sum beamforming. Furthermore, most experiments and innovations use beamforming as a measurement tool. This research aims to improve upon previous research in two ways. The first is to create an adaptable acoustic output beamformer with applications in tablet-based sound. The second is to do so in the near-field (under six feet) by utilizing a method that will be henceforth known as "point and sum" beamforming in which the signals are summed at a single point, in this case the ear of the user, instead of creating a wave-front. This should produce more accurate and controllable wave pattern beams. The feasibility of this will first be verified in simulation, using the MATLAB environment. If successful, the point and sum methodology will then be coded into VHDL for synthesization onto a Field Programmable Gate Array (FPGA). Finally a

speaker array will be designed and built to experimentally test the functionality of the system with the FPGA and its applicability to a system that maintains stereo isolation within the footprint of a tablet device.

2. Simulations

2.1 Overview of Simulation Construction

As this project focused on engineering research and development, there are no previous experiments or inventions to reference. Therefore, a simulation of the various beamforming methods was first created in MATLAB. It modeled the waveforms as sine waves and summed the magnitudes these waves to view the beams that were created over time. These simulations created results to compare against and proved the design feasible.

The purpose of simulation was to see if there was a difference in directionality and magnitude between three cases: point and sum beamforming, delay and sum beamforming, and no beamforming. Point and sum beamforming uses the Pythagorean theorem to calculate the delay based on the dimensions of the speaker array, the distance to the user and the speed of sound. On the other hand, delay and sum beamforming creates a wave-front where each delay is a multiple of the first (x, 2x, 3x … etc.) Finally, a system with no beamforming has no delays or summing built in – each wave is simultaneously driven out of each speaker. Delay and sum beamforming is shown in Figure 1 and point and sum beamforming is shown in Figure 2. Notice the distinct wavefronts being formed in Figure 1 versus the convergence that occurs in Figure 2.

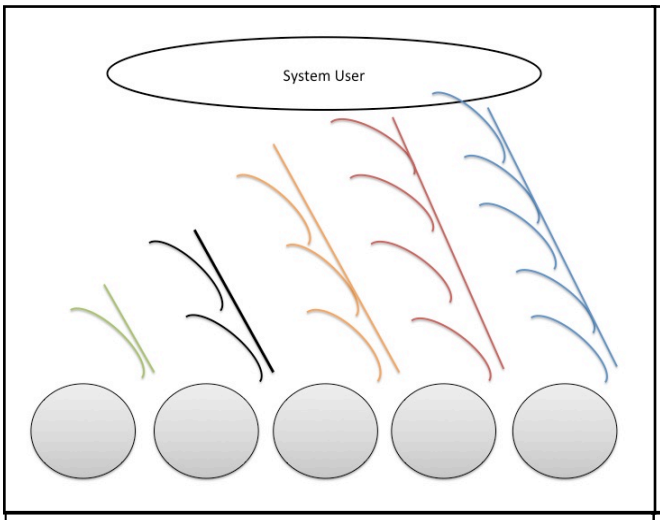

Figure 1. Shows delay and sum beamforming in far-field. Lines denote wave-fronts formed.

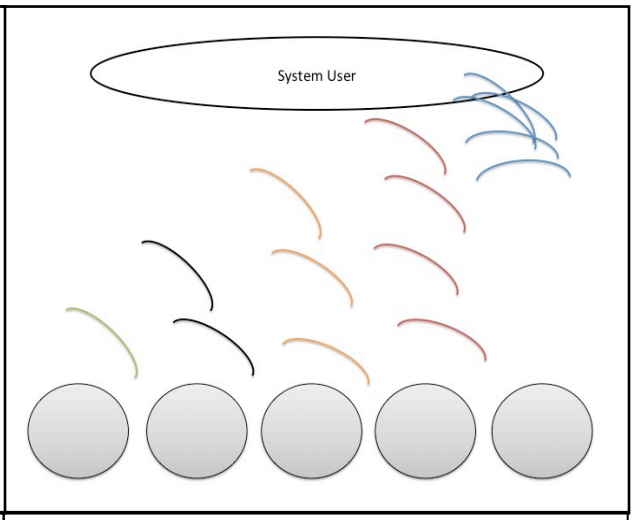

Figure 2. Shows the new near-field beamforming method, using point and sum.

This convergence in Figure 2 is important because it allows more accurate separation between the two channels, as opposed to the interference in Figure 1. Although it seems counterintutive, when the wave-fronts converge together the beam becomes more accurate – this results in superior separtation between the channels.

2.2 Simulation Design

To begin the simulations, a 30" by 30" field was constructed in simulation to mimic the field over which the waves would propagate. The five distinct sound waves, modeled as sine waves, were then created with phase shifts in the x-direction (-4, -2, 0, 2, 4) based on the position of each transmitter modeled. The delay of each wave creates beamforming by implementing phase shifts in the y-direction. *Omega* (ω) controls the period of the function, which in turn is dependent on the frequency. The signal *phase_shift* controls the phase shift of every signal together, which is used to measure signal strength over time. An example equation of all three is below:

$$z_{point\ and\ sum} = \sin(\omega * \sqrt{(x+4)^2 + (y-1.2982)^2} + phase\_shift) \quad (1)$$

$$z_{delay\ and\ sum} = \sin(\omega * \sqrt{(x+4)^2 + (y-4)^2} + phase\_shift) \quad (2)$$

$$z_{no\ beamforming} = \sin(\omega * \sqrt{(x+4)^2 + (y-0)^2} + phase\_shift) \quad (3)$$

Each of the equations above corresponds to one of the three different types of beamforming tested. The main difference between Equations 1, 2 and 3 is the term modifying the y-coordinate - which is the difference in distance that each wave has to travel and represents the delay. By changing (ω) it was possible to sweep through the frequency domain and by changing (*phase_shift*) it was possible to sweep across the time domain to find the total magnitude of the wave.

These variables made it feasible to sweep across both time and frequency domains to test each method of beamforming in MATLAB, but a method was needed to determine which signal was the most powerful and had the most separation between channels. To find this, the width of the beam was measured in each case. First, an algorithm was written to find the maximum value in the field, which became *z_max*. In order to find the point where the sound was no longer audible, which leads to the width of the beam, an edge finder method was developed based on

the logarithmic properties of hearing and decibels. Solving Equation 4 leads to Equation 5, which gives a formula for sound in decibels versus magnitude of signal. Sound was considered inaudible when it was half of the magnitude of the maximum signal as seen in Equation 6.

$$L_{decibel} = log_{10}(magnitude) \quad (4)$$

$$10^{L} = magnitude \quad (5)$$

$$for\ \frac{L}{2}\ then\ 5^{\frac{L}{2}} = \sqrt{magnitude} \quad (6)$$

The method shown in Equation 6 calculates both the separation of the beam being created in each of the three cases across time and frequency domains.

2.3 Simulation Results

Simulations were created across both frequency and time to show the beam pattern. Graphical representations can be seen in **2.4 Simulation Graphics**. Although these results seemed to support point and sum beamforming as the best method in the near field, there were no quantitative data to support this conclusion. As discussed above, an edge-finder method was implemented in MATLAB to find where the data reached half of the desired magnitude. After finding all of these points, another method measured the distance between each of these instances. This gives the width of each beam of high signal and low signal. From these results the separation of the two channels and the strength of each individual channel were clear. This was repeated for each of the three beamforming methods being compared.

Overall, the data follows trends predicted. There was never any separation between channels in the no beamforming testing. The far-field testing showed its lack of precision; demonstrated in the wild oscillations present in the data. No trend could be extrapolated from the data collected. However, the data collected for the near-field shows a well-functioning system with a minimum signal separation of 2 inches and a minimum beam width of 2 inches, which allows for the signal to stay separated and receivable by the chosen receiver.

As these results were found in simulation, they are assumed to model the system correctly. Therefore it was assumed that there was an indiscernible amount of experimental error present. However, some sources of error could have been introduced with the rounding used in the signal-width approximator method. As this error was constant across all cases tested and only the differences between the three are being analyzed, this error can be disregarded. Visual

representations of simulations conducted and the data extracted from these simulations are shown below. Each page includes a snap shot in time for 3000 Hz (Figure 3 for point and sum, Figure 6 for delay and sum and Figure 9 for no beamforming), then a summation of the total signal magnitude change over time at 3000 Hz (Figure 4 for point and sum, Figure 7 for delay and sum and Figure 10 for no beamforming) and finally a scatter plot (Figures 5, 8 and 11) of the separation between the high and low signals across frequencies.

2.4 Simulation Graphics

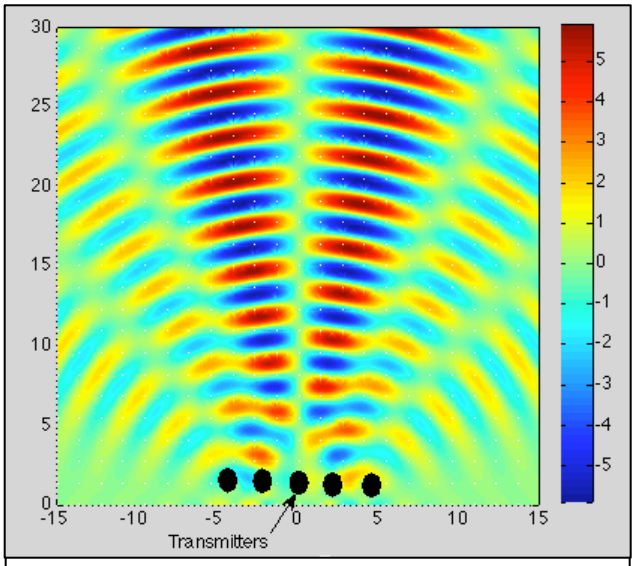

Figure 3. 3D MATLAB plot of the near-field simulations using point and sum beamforming at 3000 Hz.

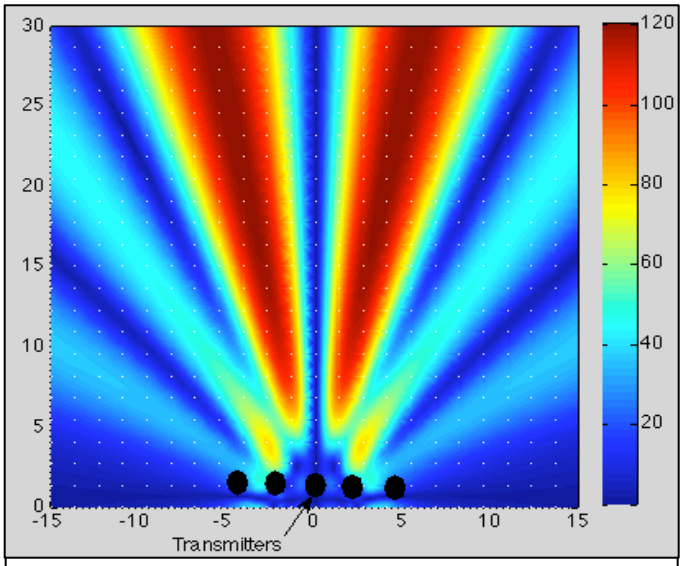

Figure 4. A MATLAB plot in the near-field of the total difference in sound over time at 3000 Hz**,** which is the audible sound.

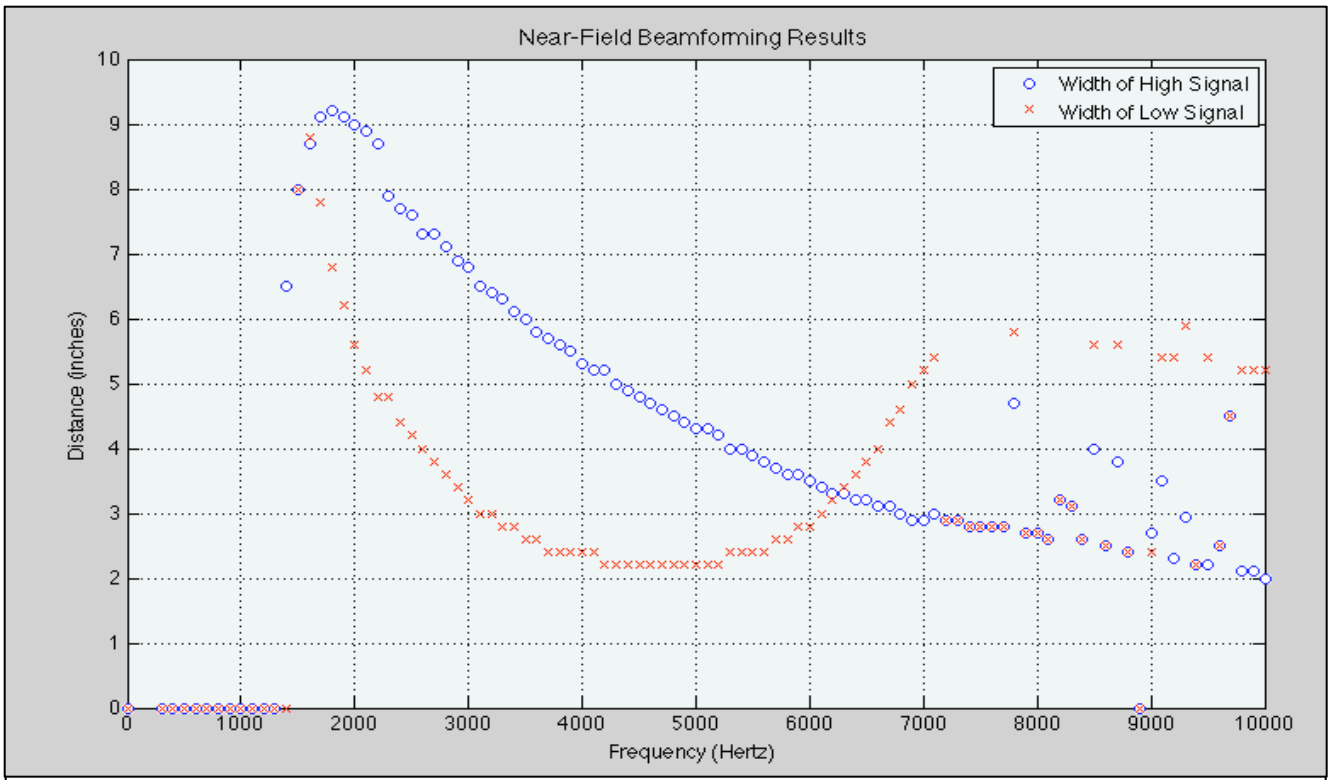

Figure 5. Plot of the quantitative beam widths measured. The *no sound* line is more important as it shows the separation distance between the two channels measured.

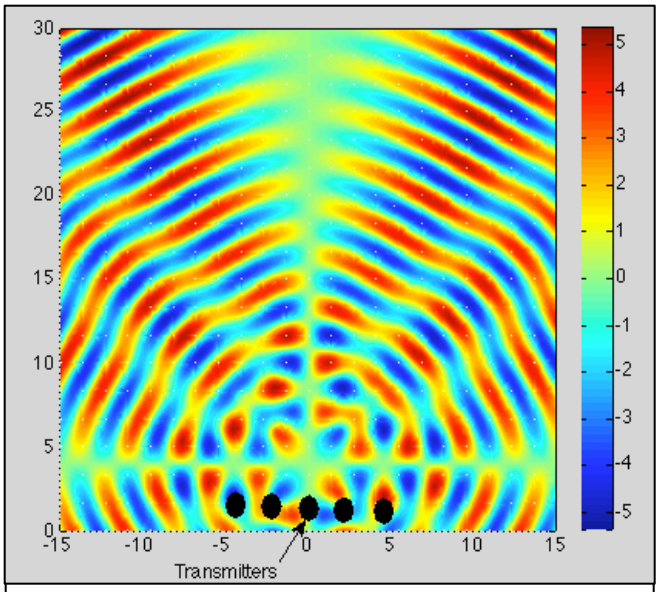

Figure 6. 3D MATLAB plot of the far-field simulations using delay and sum beamforming at 3000 Hz.

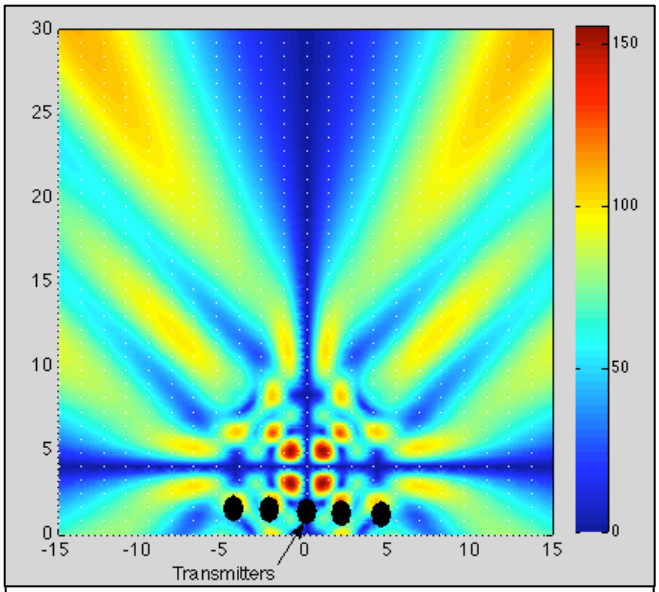

Figure 7. A MATLAB plot in the far-field of the total difference in sound over time at 3000 Hz**,** which is the audible sound.

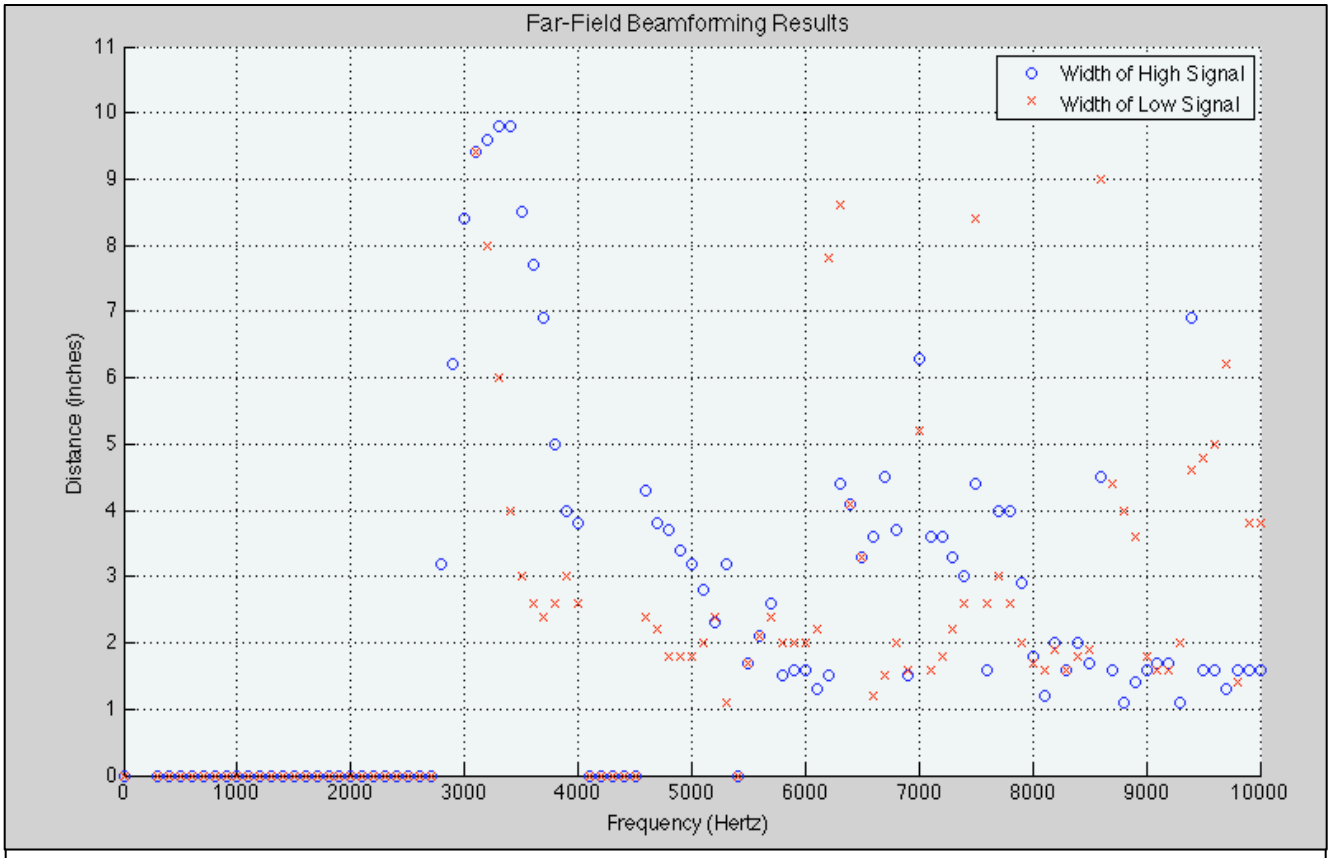

Figure 8. Plot of the quantitative beam widths measured. The *low signal* data is more important as it shows the separation distance between the two channels measured.

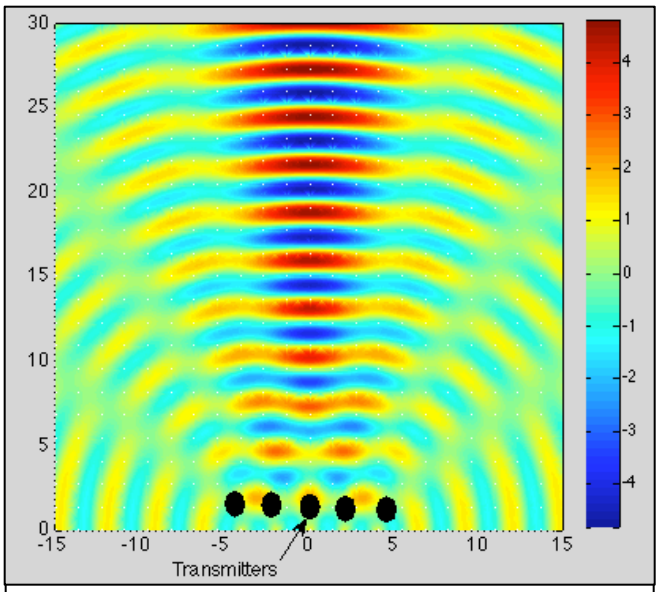

Figure 9. 3D MATLAB plot of simulations without beamforming at 3000 Hz.

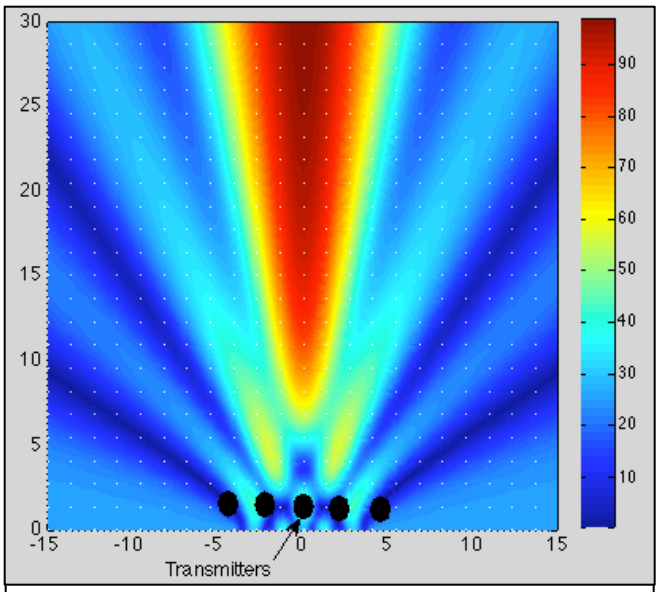

Figure 10. A MATLAB plot of the total difference in sound over time at 3000 Hz**,** without beamforming.

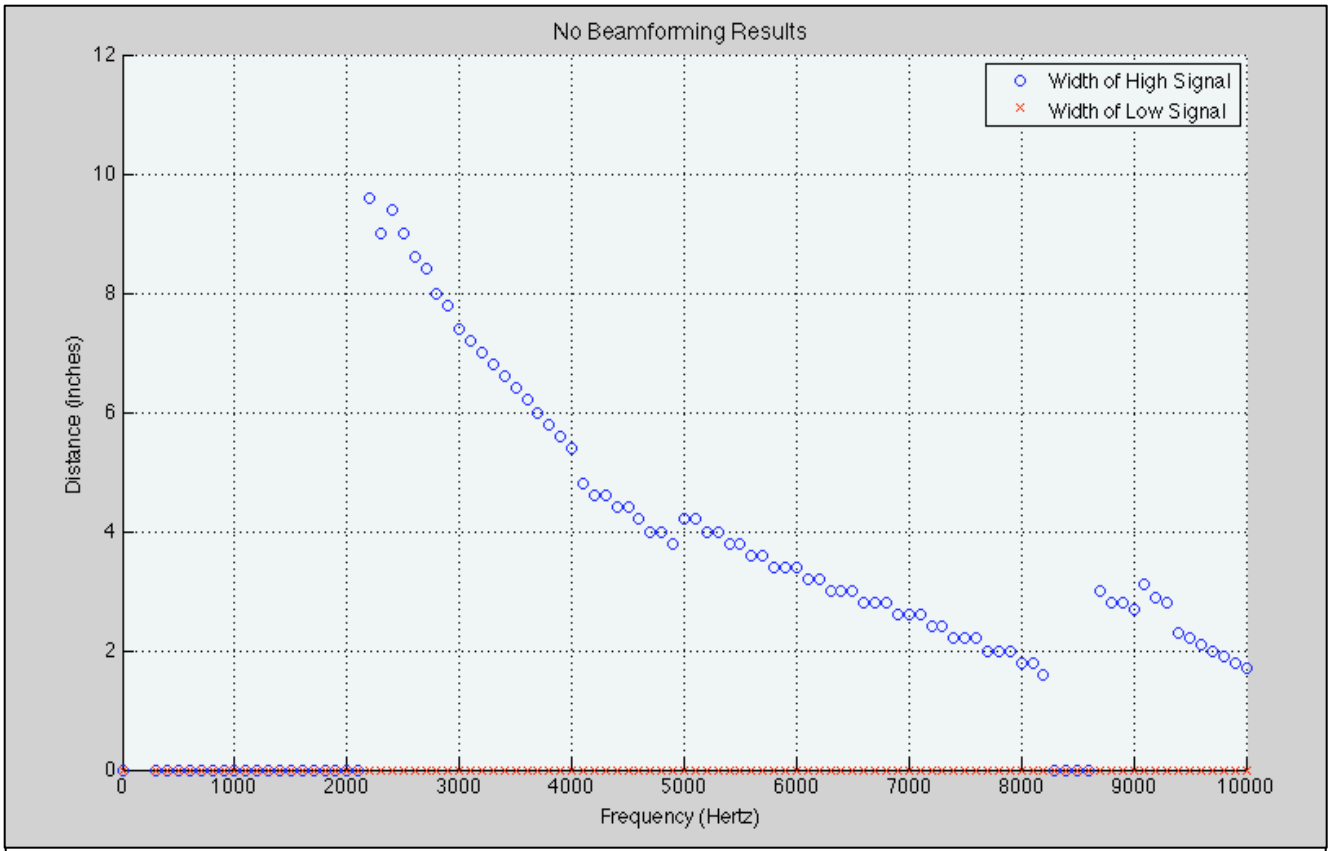

Figure 11. Plot of the quantitative beam widths measured. The *no sound* line is more important as it shows the separation distance between the two channels measured.

3. Hardware Design

3.1 VHDL Code Development

Although the point and sum methodology had been developed in simulation, it also required testing in hardware to confirm its functionality for acoustic applications. The processing hardware (FPGA design) was written in Very High Speed Integrated Circuit Hardware Description Language (VHDL) with four main processes: the delay calculator, clock division, data processing and an output selector. A block diagram is shown in Figure 12.

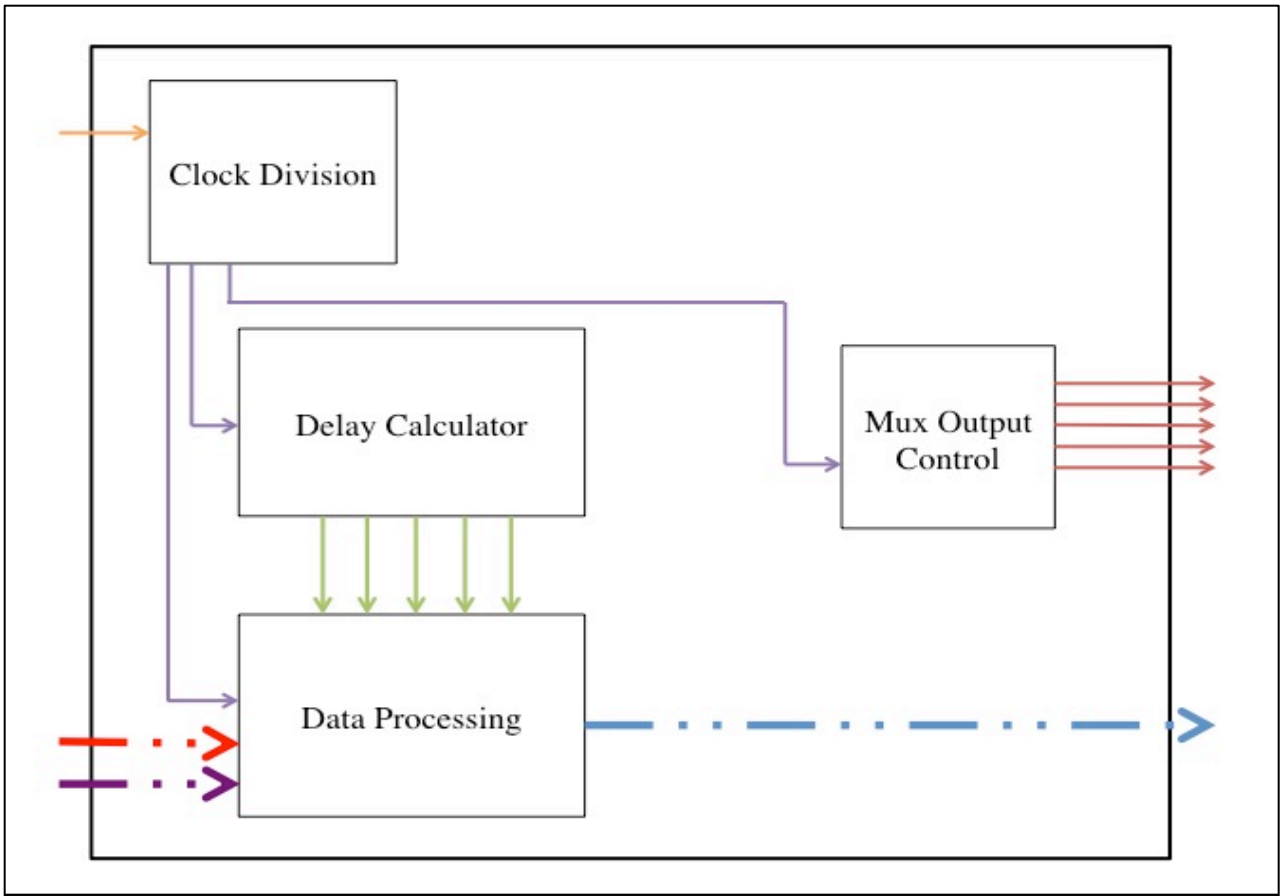

Figure 12. VHDL block diagram for the processing designed in this circuit.

The delay calculator was the most math intensive of the processes. Although the formula to calculate the delays for point and sum beamforming (which is seen below) is rather simple, the VHDL implementation is complex because VHDL does not include square root functionality.

$$delay_n = \frac{\sqrt{distance^2 + (speaker\_distance * n)^2} - distance}{speed\_sound}$$

To achieve the square root function, an iterative approach was used to approximate a square root. This was repeated four times to calculate the delays from all five speakers (the first delay was zero).

To create a clock with a period of 1 μs (named *us_clock*), a clock division was used. First a generic (name for constant in VHDL) was created with the predetermined division ratio of the system clock to the *us_clock*. This was accomplished by counting rising edges of the system clock (*i_clock*) until it equaled the generic, then inverting the current state of *us_clock.* There was also a reset command that set the edge counter back to zero and *us_clock* to zero if needed.

Based on the delays calculated, it was possible to process the input data into numbers ready for output and amplification. A shift register was created out of logic vectors (8 bit numbers for sound) to hold each sound sample. Every 23 μs (period of a 44,100 Hz clock rounded to nearest integer) a new sample was fed into the shift register and the other values shifted down one. At the same time, a counter was running from 0 to 115 to implement the near-field delays discussed above. When it reached a desired delay value that point in the shift register was stored to the appropriate speaker channel for output. This process was repeated for both the left and right channels separately. However, an output method was needed to address the lack of input and output pins on the Nexys 3 Board (Spartan 6 FPGA) used for experimentation.

Because there were not sufficient input and output pins on the FPGA to perform all operations in parallel, the data going out of the FGPA needed to be multiplexed. This was achieved in 5 μs by quickly enabling each channel individually based on a counter triggered by the rising edge of the *us_clock*. When each channel was enabled, the Digital to Analog Converter (DAC) sampled that channel via the *o_dataout* signal. Each *o_dataout* channel added a left and right channel together for instance *data_l_0* and *data_r_4* were summed together and *data_l_2* and *data_r_2* were also summed together. This 8 bit digital audio was then converted to analog through a MX7224 DAC then amplified using two LF411 operational amplifiers. Finally, using TIP 41 and TIP 42 transistors, the current was amplified to drive an Aurasound NSW1-205-8A speaker. This audio chain was created five times, one for each channel used.

After the VHDL code was completed, the FPGA was integrated into a larger system to implement the processing with DACs and speakers, as described above. The system block diagram is shown in Figure 13.

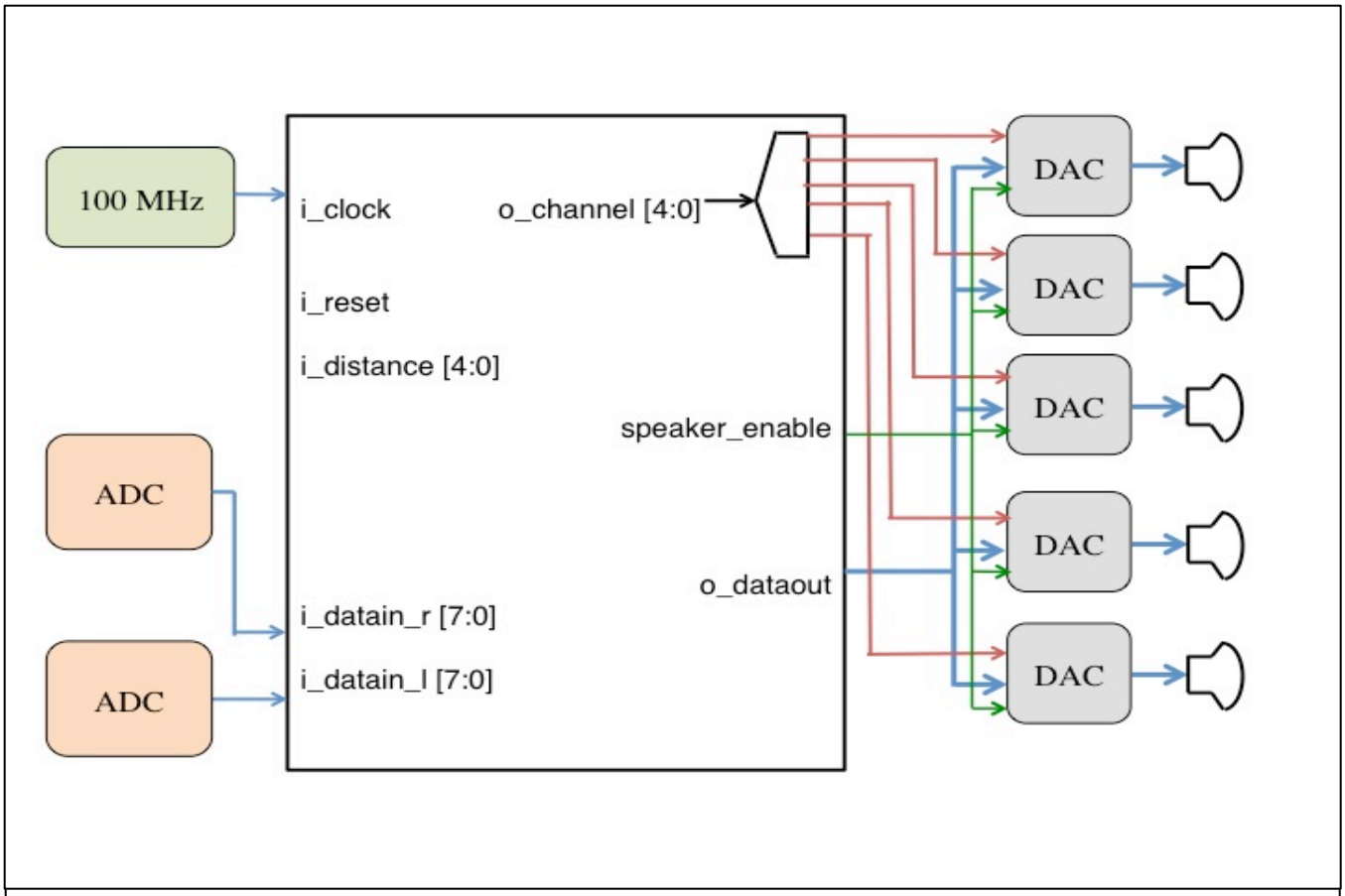

Figure 13. The block diagram above shows the high level data flow through the system. Notice the only inputs are a 100 MHz system clock and a memory block.

3.2 Creation of Speaker Hardware

A speaker enclosure was created to house the five speakers and the system. It was designed in AutoCAD then milled out to create an array of five drivers. Speakers were then installed in each of the five holes milled out. To reduce vibrations between the speakers and the solid plastic frame, rubber gaskets were placed between the two. This ensured isolation between the five drivers and the speakers in addition to reducing vibration interference between the drivers. The model that was created in AutoCAD is shown below in Figure 14. At the top of the model are the 5 congruent circular holes created for the speaker drivers that are 1.5 inches in diameter. The width of the speaker array is 10.5 inches and the height of the speaker array is 11.15 inches. It was milled out of a piece of 0.75-inch thick plastic. These dimensions were chosen because they fit the dimensions of an iPad well. In the center of the drawing there is a large cutout that represents the location of the iPad.

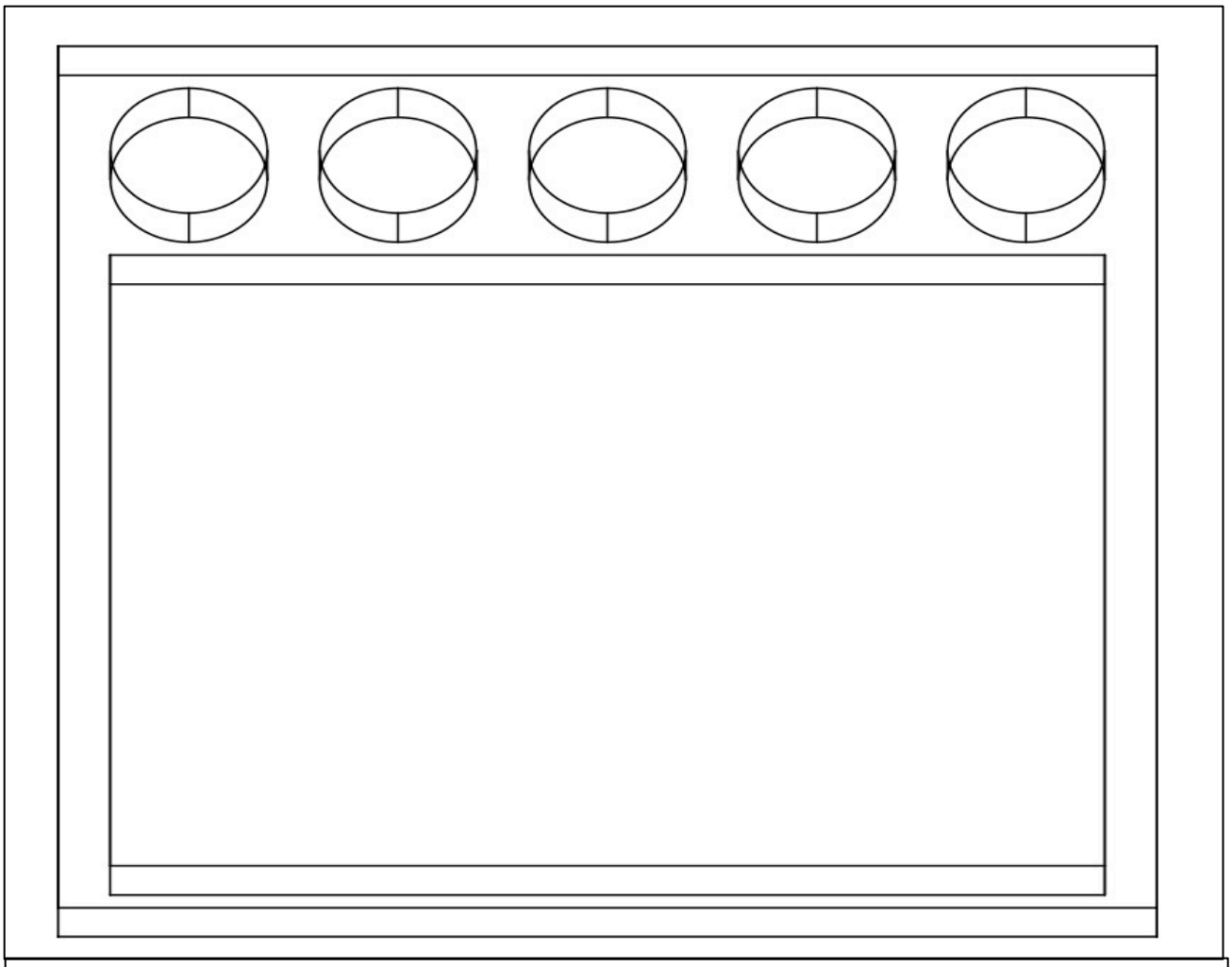

Figure 14. This shows the model created in AutoCAD that was then converted into G-Code for a Tormach CNC mill to create the speaker array in this research.

3.3 Results

After concluding that point and sum beamforming was the most accurate method in the near-field, a FPGA architecture was then developed and tested for the acoustic application described in **1. Introduction**. Early FPGA results were unsuccessful due to difficulties with keeping the multiple clocks (*i_clock, us_clock, i_sampleclock*) used synchronous. Additionally, problems using the cellular RAM on the Nexys 3 occurred. However, once clock and RAM issues were resolved, the FPGA started functioning correctly and the desired stereo effect could be heard very well.

Unfortunately, it was difficult to obtain quantitative hardware results because of the qualitative nature of audio quality and stereo separation. The best method of hearing the stereo

isolation was by playing a conversation with one voice on the left channel and one on the right channel of stereo sound; most users observed this sound isolation effect. The system was also tested with music, which stressed the frequency range of the beamformer more than the voice conversation and led to poorer results. This means that there was such a large variation in frequencies associated with music (20 to 20,000 Hertz) versus voice (300 to 3000 Hertz) that the beamformer was unable to handle every frequency in that range. So far, results with the music have not been nearly as promising as the results with the voice conversation.

Some other interesting trends were observed during testing. For instance, although most users could hear the stereo isolation being created and were impressed by the fact, some could not. This may be caused by loss of hearing in individual users or because individual users perceive and process sound differently. However, the vast majority of users could hear stereo isolation. This proves the success of both the hardware design and the underlying principles of point and sum beamforming for use in the near-field.

4. Conclusion

4.1 Discussion of Results

The simulation results address three main areas: point and sum beamforming, delay and sum beamforming, and no beamforming. Each of these methods was simulated in the near-field to find which method is the most effective in maintaining isolation between the two channels and creating the most coherent wave-forms. After determining the most effective method of beamforming in the near-field in simulation, this theory was tested on a FPGA. The FPGA results are still fairly qualitative but do indicate that the system is functioning correctly.

Results show that point and sum beamforming is the most effective in the near-field for multiple reasons. First and foremost is the amount of separation between the two channels throughout frequencies. The graphs in **2.4 Simulation Graphics** above show that the minimum separation distance between beams, or channels, is two inches for point and sum beamforming (Figure 5) versus one inch for delay and sum beamforming (Figure 5). This means that the separation acquired with delay and sum beamforming, which is a far-field technique, is far less suited to applications in the near-field. Furthermore, no beamforming (Figure 11) has the worst separation of all, which was expected. This means that no beamforming should not be used to achieve channel separation in the near-field. Another important aspect of the simulation results is

the amount of separation between channels that can be seen in Figures 3, 5, and 9. The goal was to make a precise beam, and this only occurs in Figure 3, which shows the point and sum method of beamforming. These results are far more precise than those shown in Figure 6, which uses delay and sum beamforming, and even more so than the waveforms shown in Figure 9 which has no beamforming.

These findings show that not only is it possible to create a beamformer that works well in the near-field, but that the best method is using point and sum beamforming developed as part of this research (versus the more traditional delay and sum beamforming). During this experimentation point and sum beamforming was applied to a sound system for tablet devices. This use of beamforming is unlike any other research in the field today. Not only were the results positive for point and sum beamforming in simulation, but they were also very noticeable with hardware. Many users could perceive an audio image of what was happening around them, which was the goal of experimentation. Because users could perceive an audio image, this shows that both channels were completely isolated, which proves the functionality of the design.

4.2 Conclusions

The goal of this research was to determine the best method of using beamforming in the near-field, and more specifically, its application to acoustic use in creating a speaker array that fits within the footprint of a tablet and creates an audio image. However, after a detailed literature review, there did not seem to be any suitable methods to achieving this. Because of this a new method was developed called point and sum beamforming which aimed to be much more accurate than the traditional delay and sum beamforming by creating a large lobe of sound for the listener instead of just creating a wave-front.

Simulation results were obtained to compare the three different methods of beamforming: point and sum, delay and sum, and no beamforming. All of the results obtained have been validated based on their beam pattern and the quantitative beam width data collected. Then, after confirming that point and sum beamforming was the most effective in the near-field, it was implemented into hardware using a FPGA. The hardware was then tested by recording one voice of a conversation on the right channel and the other on the left channel; based on the stereo separation between the two channels, users could imagine themselves sitting between the two voices on the conversation. Because multiple users could perceive the stereo isolation and

imaging in the system, and most users could hear the same thing, there are likely no other causes of the effect.

This research is important because it proves the concept of point and sum beamforming and its relevance to work in the near-field. All prior research in this field deals with far-field applications and how to implement at delay and sum beamformer. However, a delay and sum beamformer is not well suited to use in the near-field because it creates wave-fronts at a specific angle instead of a converging wave-front at the specified point. These innovations in point and sum beamforming have the potential to revolutionize the uses of near-field beamforming with respect to medical imaging and treatment along with the operation of cellular towers. The other improvement upon previous research was the creation of an acoustic beamformer that fits within the footprint of a tablet device. Previous research has not dealt with waves in the acoustic spectrum, but rather radio waves or forms of electromagnetic radiation such as light. The fact that this research focuses on the near-field and an acoustic output beamformer separates it from other research as few other researchers have asked similar questions.

4.3 Future Work

The largest improvement to the system would be upgrading the processing capabilities. To achieve this, much broader research must be conducted into different wave manipulation techniques. These ideas will likely be found in literature with no relation to beamforming, but which describe methods of suppressing off axis signals or more effectively summing waves. Additionally, nine drivers will be used instead of the five currently being used to allow more precise control of the system. Following the methodology set out in this research all new techniques will be tested in simulation against the current most effective method and then described in VHDL and synthesized onto hardware for physical testing.

To further refine the conclusions, a more effective method needs to be developed to more precisely quantify the results. This could include more detailed measurement or an entire microphone array to measure the sound levels at various locations. Furthermore, the system needs to be tested at various distances and frequencies to completely prove that it is functioning correctly. In the future, the system needs to be shrunk down to the consumer electronics scale for widespread testing and data collection. Additionally, sensors will be added to perceive distance, instead of switches that hard code the device into a certain distance mode. A possible option is a

sonar sensor, which costs relatively little, and returns data that is simple to analyze and map out the distance to the user.

Applications of point and sum beamforming are not only limited to speaker arrays that aim to enhance the stereo image perceived by a listener. It can be used to maximize the power out of a single cell tower antenna, by more effectively delivering signals to users very close to the tower. Another application is using it for medical imaging or targeted radiation, as it allows a greater degree of control and precision versus delay and sum beamforming. The applications and further work abound for point and sum beamforming in the near-field, and show promise as this research has shown.

5. References

Buckingham, M. J. (1994). On Surface-Generated Ambient Noise in an upward Refracting Ocean. *Philosophical Transactions: Physical Sciences and Engineering*, *346*(1680), 321-352.

David, E. E., Jr. (1961). Reproduction of Sound. *Scientific American*, 72-85.

Deller, A. T., Brisken, W. F., Phillips, C. J., Morgan, J., Alef, W., Capallo, R., . . . Wayth, R. (2011). DiFX-2: A More Flexible, Efficient, Robust, and Powerful Software Correlator. *Publications of the Astronomical Society of the Pacific*, *123*(901), 275-287.

Greenwood, K. (2011). Understanding Passive Beamforming Networks. *Defense Electronics*, 18-24.

Hagan, C. C., Woods, W., Johnson, S., Calder, A. J., Green, G. G.R., & Young, A. W. (2009). MEG Demonstrates a Supra-Additive Response to Facial and Vocal Emotion in the Right Superior Temporal Sulcus. *Proceedings of the National Academy of Sciences of the United States of America*, *106*(47), 20010-20015.

Hinich, M. (1977). Array Design for Measuring Source Depth in a Horizontal Waveguide. *SIAM Journal on Applied Mathematics*, *32*(4), 800-806.

Horning, S. S. (2004). Engineering the Performance: Recording Engineers, Tacit Knowledge and the art of Controlling Sound. *Social Studies of Science*, *34*(5), 703-731.

Kendall, G. S. (1995). A 3-D Sound Primer - Directional Hearing. *Computer Music Journal*, *19*(4), 23-46.

Kendall, G. S. (1995). The Decorrelation of Audio Signals and Its Impact on Spatial Imagery. *Computer Music Journal*, *19*(4), 71-87.

Manz, B. (2012, September 20). Is EW ready for AESA (and vice versa)? *Journal of Electronic Defense*.

Moore, F. R. (1983). A General Model for Spatial Processing of Sounds. *Computer Music Journal*, *7*(3), 6-15.

Park, S., Karpiouk, A. B., Aglyamov, S. R., & Emelianov, S. Y. (2008). Adaptive beamforming for photoacoustic imaging. *Optical Society of America*, *33*(12), 1291-1293.

Pollack, L., & Weiss, H. (1984). Communications Satellites: Countdown for INTELSAT VI. *Science, New Series*, *4636*(223), 553-559.

Rulkov, N. F., Tsimring, L., Larsen, M. L., & Gabbay, M. (2006). Synchronization and beamforming in an array of repulsively coupled oscillators. *Physical Review*, *74*, 1-10.

Simonetti, F., & Huang, L. (2009). Synthetic aperture diffraction tomography for three-dimensional

imaging. *Proceedings: Mathematical, Physical and Engineering Sciences*, *465*(2109), 2877-2895.

Spadoni, A., Daraio, C., & Freund, L. B. (2010). Generation and control of sound bullets with a nonlinear acoustic lens. *Proceedings of the National Academy of Sciences of the United States of America*, *107*(16), 7230-7234.

Williams, J. F. (1984). Review Lecture: Anti-Sound. *Proceedings of the Royal Society of London.Series A, Mathematical and Physical Sciences*, *395*(1808), 63-88.